Thermal quenching of photoluminescence from Er-doped GaN thin films

J.T. Seo[a,*], U. Hömmerich[a], D.C. Lee[b], J. Heikenfeld[b], A.J. Steckl[b], J.M. Zavada[c]

[a]*Research Center for Optical Physics, Department of Physics, Hampton University, Hampton, VA 23668, USA*
[b]*Nanoelectronics Laboratory, University of Cincinnati, Cincinnati, OH 45221, USA*
[c]*US ARL—European Research Office, London NW1 5TH, UK*

Abstract

The green (537 and 558 nm) and near infrared (1.54 μm) photoluminescence (PL) spectra of Er-doped GaN thin films have been investigated as a function of temperature, excitation wavelength, and pump intensity. Thermal quenching measurements showed that the integrated green Er^{3+} PL intensity ($^4S_{3/2}/^2H_{11/2} \rightarrow {}^4I_{15/2}$) remained nearly constant up to 150 K, but decreased at higher temperatures due to a less efficient Er^{3+} excitation. The integrated infrared Er^{3+} PL intensity ($^4I_{13/2} \rightarrow {}^4I_{15/2}$) was found to be temperature-independent up to 250 K, but decreased slightly at higher temperatures due to the onset of non-radiative decay. Pump intensity PL studies revealed that the above-gap excitation cross-section is more than two orders of magnitude greater than the below-gap excitation cross-section. Within a simplified three-level model, the above-gap excitation cross-section was estimated to be $\sim 10^{-16}$ cm^2. This result indicates that Er^{3+} ions can be excited efficiently through carrier-mediated processes in a forward-biased GaN:Er light emitting device. © 2002 Elsevier Science B.V. All rights reserved.

Keywords: Er-doped GaN; Luminescence spectroscopy; Thermal quenching

1. Introduction

Er-doped Si and III–V semiconductors have been studied for over a decade for possible applications in optoelectronics. The development of practical, Si-based light emitting devices, however, has been severely limited by a low Er^{3+} concentration and strong quenching of the infrared (IR) Er^{3+} luminescence at 1.54 μm [1–3]. A major breakthrough in this research area was the observation of intense room-temperature Er^{3+} photoluminescence (PL) at 1.54 μm from Er-doped wide-gap semiconductors [2–4]. The Er^{3+} PL quenching in these material systems was reported to be less than a factor of two between 15 K and room temperature. GaN thin films doped with rare earth elements (Er, Eu, Tm, etc.) have recently attracted much attention due to the development of visible (blue, green, red) and infrared electroluminescent devices [5]. These rare earth-doped thin films are currently being intensively studied for possible applications in full color displays and optical communications [5–8].

In this paper, we present spectroscopic results on Er-doped GaN thin films prepared by solid source molecular beam epitaxy (SSMBE). The investigations focused on PL studies as a function of excitation wavelength, temperature, and pump intensity. The measured data are discussed in terms of the Er^{3+} excitation and de-excitation processes in GaN.

2. Experimental

The Er-doped GaN films were grown by SSMBE on Si substrates, as described previously [6]. The Er concentration was determined to be $\sim 2 \times 10^{20}$ cm^{-3} (~ 0.2 at.%) based on SIMS and RBS analyses. This concentration is well below the limit of luminescence concentration quenching (~ 1 at.%) recently reported [7]. The PL studies were performed using UV (336–363 nm) or visible (496.5 nm) lines of an Argon ion laser. The PL spectra were recorded using a 1-m monochromator equipped with either an InGaAs detector or photomultiplier tube. The PL signal was processed using lock-in techniques. PL lifetime studies employed the 355-nm line of a Nd:YAG laser for excitation. The lifetime transients were averaged using a digitizing oscilloscope.

*Corresponding author.
E-mail address:* jaetaeseo@hotmail.com (J.T. Seo).

Report Documentation Page

1. REPORT DATE **2002**	2. REPORT TYPE	3. DATES COVERED **00-00-2002 to 00-00-2002**

4. TITLE AND SUBTITLE	5a. CONTRACT NUMBER
Thermal quenching of photoluminescence from Er-doped GaN thin films	5b. GRANT NUMBER
	5c. PROGRAM ELEMENT NUMBER
6. AUTHOR(S)	5d. PROJECT NUMBER
	5e. TASK NUMBER
	5f. WORK UNIT NUMBER

7. PERFORMING ORGANIZATION NAME(S) AND ADDRESS(ES) **University of Cincinnati,Nanoelectronics Laboratory,Cincinnati,OH,45221-0030**	8. PERFORMING ORGANIZATION REPORT NUMBER

9. SPONSORING/MONITORING AGENCY NAME(S) AND ADDRESS(ES)	10. SPONSOR/MONITOR'S ACRONYM(S)
	11. SPONSOR/MONITOR'S REPORT NUMBER(S)

12. DISTRIBUTION/AVAILABILITY STATEMENT
Approved for public release; distribution unlimited

13. SUPPLEMENTARY NOTES

14. ABSTRACT

15. SUBJECT TERMS

16. SECURITY CLASSIFICATION OF:			17. LIMITATION OF ABSTRACT	18. NUMBER OF PAGES	19a. NAME OF RESPONSIBLE PERSON
a. REPORT **unclassified**	b. ABSTRACT **unclassified**	c. THIS PAGE **unclassified**		**5**	

3. Results and discussion

The PL spectra of GaN:Er, measured at room temperature, using above-gap (336–363 nm) and below-gap (496.5 nm) excitation are shown in Fig. 1. With above-gap pumping, three PL features can clearly be distinguished (Fig. 1a): the band-edge signal from GaN located at ~369 nm, a defect-related yellow-band PL centered at ~550 nm, and several intra-4f Er^{3+} transitions. The intra-4f Er^{3+} transitions are identified as: 537 nm ($^2H_{11/2} \rightarrow {}^4I_{15/2}$), 558 nm ($^4S_{3/2} \rightarrow {}^4I_{15/2}$), 667 nm ($^4F_{9/2} \rightarrow {}^4I_{15/2}$), 1000 nm ($^4I_{11/2} \rightarrow {}^4I_{15/2}$), and 1540 nm ($^4I_{13/2} \rightarrow {}^4I_{15/2}$). With below-gap pumping, only the intra-4f Er^{3+} emissions were observed (Fig. 1b). It is important to note that the Er^{3+} PL lines exhibited slightly different fine-structures and linewidths for the two excitation wavelengths suggesting the existence of different Er^{3+} sites in GaN [8,9].

In Fig. 2, the integrated Er^{3+} PL intensity and the PL lifetime for the infrared (1540 nm) line are plotted as a function of the sample temperature. The PL measurements were taken using above-gap excitation. Compared to narrow-gap semiconductors such as Si or GaAs [1,2], the integrated infrared PL intensity from GaN:Er was remarkably stable. Thermal quenching was less than a factor of two between 15 K and room temperature. At higher temperatures, the integrated IR PL started to decrease and was reduced by a factor of ~3 at 500 K relative to its low temperature value.

A similar behavior was observed for the integrated green Er^{3+} PL intensity of the green (537 and 558 nm) lines, as

shown in Fig. 3. With above-gap excitation, the integrated green PL intensity ($^4S_{3/2} / {}^2H_{11/2} \rightarrow {}^4I_{15/2}$) remained nearly constant up to only ~150 K, and then decreased at higher temperatures. At 500 K, the integrated green PL intensity was reduced by a factor of ~3 relative to its low temperature value. Since above-gap excitation generated a broad yellow band emission ~550 nm, it was difficult to measure the lifetime of the green lines. Consequently, below-gap excitation was used and the PL lifetime was measured at 558 nm. As shown in Fig. 3, the green Er^{3+} PL lifetimes follow the change in the associated integrated green Er^{3+} PL intensity very closely.

In order to interpret these results, consider the temperature dependence of the PL intensity at low pump power [10]:

$$I_{PL} \sim \sigma_{ex} \cdot \frac{w_r}{w_r + w_{nr}} = \sigma_{ex} w_r \tau \qquad (1)$$

where σ_{ex} is the excitation cross-section, w_r is the radiative decay rate, w_{nr} is the non-radiative decay rate, and τ is the PL lifetime ($\tau^{-1} = w_r^{-1} + w_{nr}^{-1}$). As discussed previously [8], the green emission lifetime is reduced with increasing temperature because of the thermalization of the $^4S_{3/2}$ and $^2H_{11/2}$ excited states, which are separated by only ~700 cm^{-1}. Therefore, the $^2H_{11/2}$ state is populated only at higher temperatures. This thermalization reduces the average green PL lifetime of ~11.2 μs at 15 K to ~6.2 μs at 300 K. At 500 K, the average green PL lifetime is further reduced to less than 3 μs. The reduction in PL lifetime reflects the increase in the radiative decay rate (w_r) at
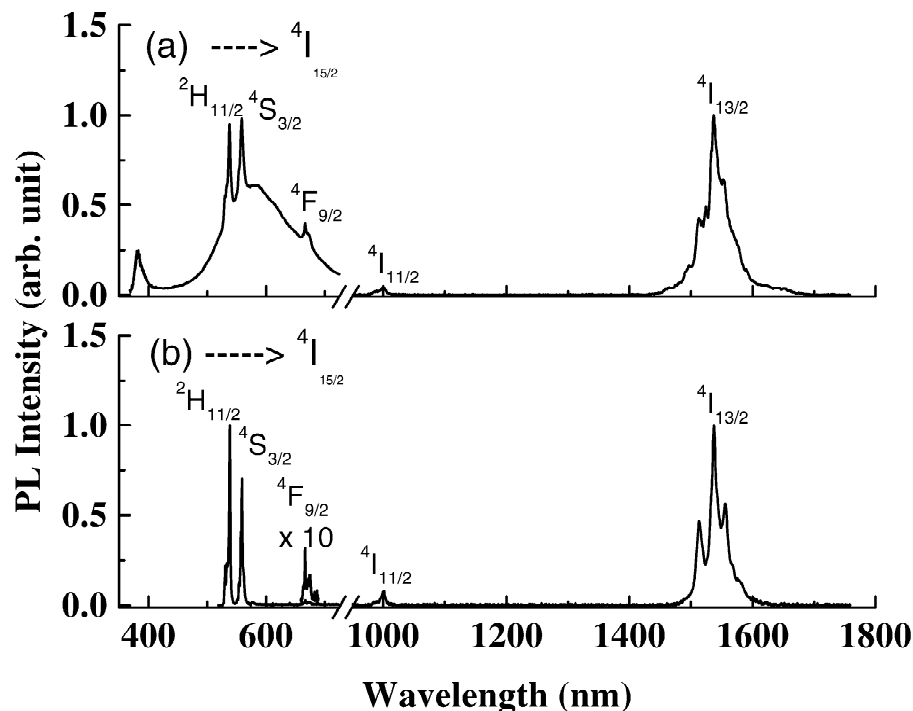

Fig. 1. Visible and infrared photoluminescence spectra of GaN:Er (SSMBE) at room temperature, (a) above-gap excitation (336–363 nm); (b) below-gap excitation (496.5 nm). The Er^{3+} transitions are indicated by their initial state. All transitions terminate in the $^4I_{15/2}$ ground state.
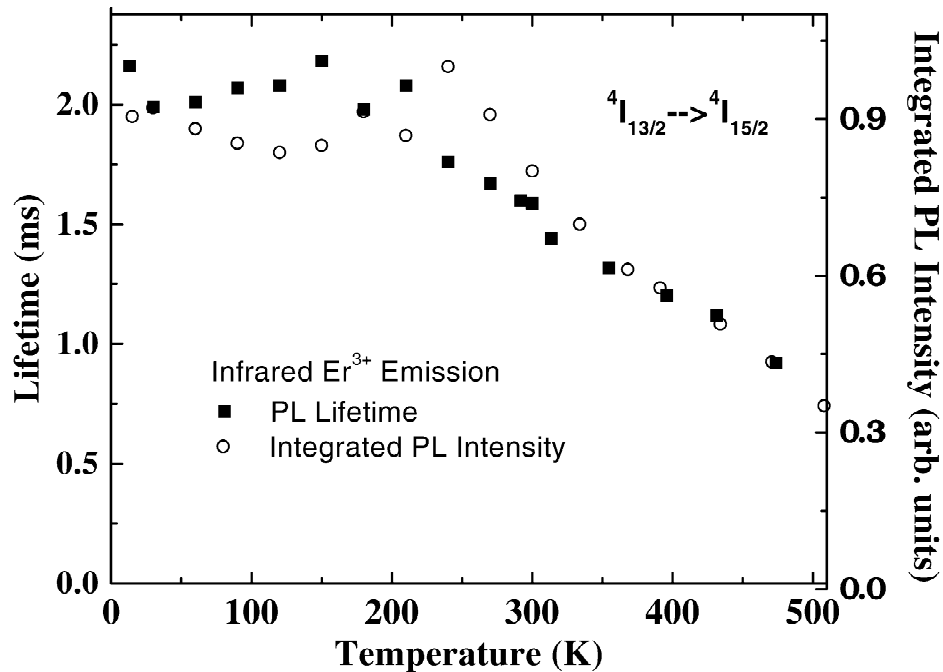
Fig. 2. Comparison of the temperature dependence of the integrated PL intensity and the PL lifetime for the infrared transition of Er^{3+} in GaN ($^4I_{13/2} \rightarrow {}^4I_{15/2}$).

higher temperatures. Assuming that non-radiative decay processes are negligibly small for the green Er^{3+} PL, the decrease in the integrated green Er^{3+} PL intensity above ~150 K is attributed to a change in excitation efficiency.

The IR Er^{3+} PL lifetime at low temperatures was measured to be ~2.1 ms and decreased to 1.6 ms at 300 K. At 500 K, the IR Er^{3+} PL lifetime was reduced to ~0.4 ms. In contrast to the green Er^{3+} PL lifetime, it can be assumed that the radiative decay rate of the ($^4I_{13/2} \rightarrow {}^4I_{15/2}$) transition is constant. Therefore, any
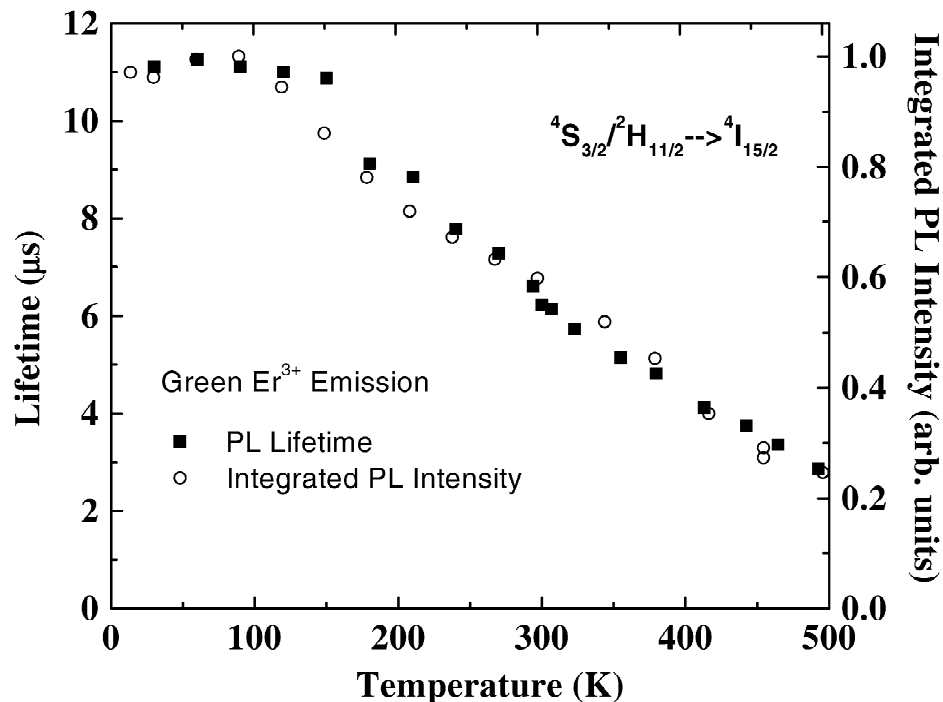

Fig. 3. Comparison of the temperature dependence of the integrated PL intensity and the PL lifetime for the green transitions of Er^{3+} in GaN ($^4S_{3/2}/{}^2H_{11/2} \rightarrow {}^4I_{15/2}$).

decrease in IR Er^{3+} PL lifetime is attributed to the onset of nonradiative decay, which consequently decreased the integrated PL intensity at higher temperatures. The detailed mechanisms of this non-radiative decay process are still under investigation.

To gain further insight into the excitation mechanism of Er^{3+} ions in GaN, studies of the dependence of the PL intensity on the pump intensity, at different excitation wavelengths, were performed. The behavior of integrated IR Er^{3+} PL intensity, using above-gap and below-gap excitation, is depicted in Fig. 4. With above-gap pumping (350 nm), the IR Er^{3+} PL intensity starts to saturate at pump intensities of less than 2 W/cm^2. In contrast, with below-gap excitation (514 nm), the IR Er^{3+} PL intensity increased nearly linearly with increasing pump intensity and saturation was not observed even at pump intensities as high as 150 W/cm^2 (the experimental limit). It can further be noticed that the saturation levels are different for both excitation schemes. A similar pump intensity dependence was observed for the green Er^{3+} PL for both above- and below-gap excitation.

The pump intensity-dependent PL data were modeled within a simplified three-level Er^{3+} energy scheme [10,11]. After balancing the rates of excitation and de-excitation under steady state pumping conditions, it can be shown that the pump intensity dependence of the IR Er^{3+} PL is given by:

$$I_{PL} = \frac{I_{PL,max}}{1 + \dfrac{\tau^{-1}hc}{\sigma_{ex}p_{ex}\lambda_{ex}}} \qquad (2)$$

where $I_{PL,max}$ is the maximum PL intensity, h is the Planck's constant, c is the speed of light, p_{ex} is the pump power, and λ_{ex} is the excitation wavelength. The maximum attainable PL at high pump intensity (saturation level) is given by: $I_{PL,max} = C \cdot N_{Er} \cdot w_r$, where N_{Er} is the concentration of optically active Er^{3+} ions, and C is the collection factor of the PL set-up. Fitting the experimental data to Eq. (2), an estimate of the excitation cross-section σ_{ex} can be obtained. For below-gap pumping, the fitting yielded: $\sigma_{ex} \sim 2 \times 10^{-19}$ cm^2 and $I_{PL,max} = 0.41$ with $\lambda_{ex} = 514$ nm and $\tau = 1.6$ ms being fixed parameters. This value for the below-gap excitation σ_{ex} seems reasonable compared to the cross-sections of Er^{3+} transitions in other host materials ($\sim 10^{-20}$ cm^2) [12]. The slightly higher Er^{3+} cross-section in GaN:Er could be due to defect-related Er^{3+} excitation, which overlaps the resonant Er^{3+} excitation [13]. For above-gap pumping, the best-fit of the data to Eq. (2) yielded: $\sigma_{ex} \sim 1 \times 10^{-16}$ cm^2 and $I_{PL,max} = 0.15$ with $\lambda_{ex} \sim 350$ nm and $\tau = 1.6$ ms being fixed parameters. The best-fit result indicates that the above-gap excitation σ_{ex} is more than two orders of magnitude larger than that obtained for below-gap pumping. This value for the above-gap σ_{ex} is comparable to impact excitation cross-sections reported for Er-doped GaN [14] and Er-doped Si [15] in electroluminescent devices under reverse bias.

4. Summary and conclusions

Intense green (~ 537, 558 nm) and infrared (1.54 μm) PL was observed at room-temperature from Er-doped GaN
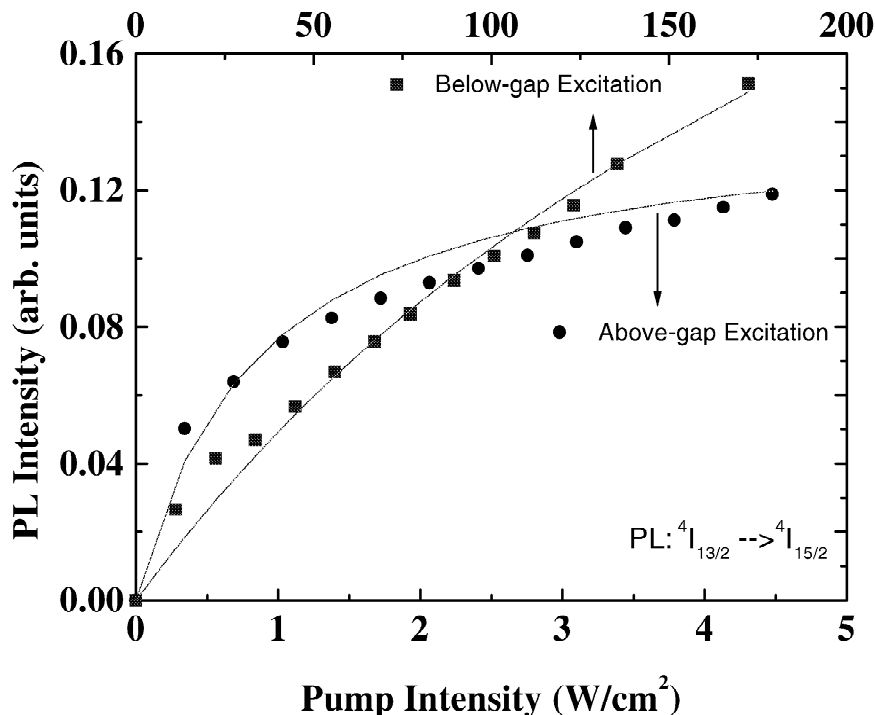

Fig. 4. Pump intensity dependence of the infrared PL from GaN:Er for above-gap and below-gap excitation. It is important to note the different pump intensity scales for the two excitation schemes. The solid lines are the best fits to Eq. (2).

thin films. Temperature-dependent PL studies have shown that quenching of the integrated green Er^{3+} PL, observed at elevated temperatures (>150 K), was due to a decreasing excitation cross-section. However, the quenching of the infrared Er^{3+} PL, above 250 K, was assigned to an increase in nonradiative decay. Pump intensity-dependent PL studies revealed that the above-gap excitation cross-section is on the order of $\sim 1 \times 10^{-16}$ cm^2. The present results suggest that an efficient Er^{3+} excitation process through carrier injection in a forward-biased light emitting diode should be possible.

Acknowledgements

References

[1] G.S. Pomrenke, P.B. Klein, D.W. Langer (Eds.), Rare Earth Doped Semiconductors I, Mater. Res. Soc., 301, 1993.

[2] S. Coffa, A. Polman, R.N. Schwartz (Eds.), Rare Earth Doped Semiconductors II, Mater. Res. Soc., 422, 1996.

[3] J.M. Zavada, T. Gregorkiewicz, A.J. Steckl (Eds.), Rare Earth Doped Semiconductors III, Mater. Sci. Eng. B, 81, 2001.

[4] J.M. Zavada, M. Thaik, U. Hommerich, J.D. MacKenzie, C.R. Abernathy, S.J. Pearton, R.G. Wilson, J. Alloys Comp. 300–301 (2000) 207.

[5] A.J. Steckl, J.M. Zavada, MRS Bull. 24 (9) (1999) 33.

[6] A.J. Steckl, R. Birkhahn, Appl. Phys. Lett. 73 (1998) 1702.

[7] D.S. Lee, J. Heikenfeld, A.J. Steckl, U. Hömmerich, J.T. Seo, A. Braud, J. Zavada, Appl. Phys. Lett. 79(6) 6 Aug 2001.

[8] U. Hömmerich, J.T. Seo, C.R. Abernathy, A.J. Steckl, J.M. Zavada, Mater. Sci. Eng. B 81 (2001) 116.

[9] A.M. Mitofsky, G.C. Papen, S.G. Bishop, D.S. Lee, A.J. Steckl, http://www.mrs.org/, 2000 Fall MRS Proceedings, 639 (2000) G6.26.

[10] S. Coffa, G. Franzo, F. Priolo, A. Polman, R. Serna, Phys. Rev. B 49 (1998) 4443.

[11] S.W. Roberts, G.J. Parker, M. Hempsted, Opt. Mater. 6 (1996) 99.

[12] S.A. Payne, L.L. Chase, L.K. Smith, W.L. Kway, W.F. Krupke, IEEE J. Quantum Electron. 28 (1992) 2619.

[13] M. Thaik, U. Hommerich, R.N. Schwartz, R.G. Wilson, J.M. Zavada, Appl. Phys. Lett. 71 (1997) 2641.

[14] J.T. Torvik, C.H. Qui, R.J. Feuerstein, J.I. Pankove, F. Namavar, J. Appl. Phys. 81 (1997) 6343.

[15] S. Wang, A. Eckau, E. Neufeld, R. Carius, Ch. Buchal, Appl. Phys. Lett. 71 (1997) 2824.